Optimal mechano-electric stabilization of cardiac alternans

Stevan Dubljevic[†] and Panagiotis Christofides[‡]

[†]Cardiovascular Research Laboratories

David Geffen School of Medicine

University of California, Los Angeles, CA, 90095

[‡]Department of Chemical and Biomolecular Engineering

University of California, Los Angeles, CA 90095

Abstract— **Alternation of normal action potential morphology in the myocardium is a condition with a beat-to-beat oscillation in the length of the electric wave which is linked through electromechanical coupling to the cardiac muscle contraction, and is believed to be the first manifestation of the onset of life threatening ventricular arrhythmias and sudden cardiac death. In this work, the effects of electrical and mechanical stimuli are utilized in alternans annihilation problem. Electrical stimuli that alter the action-potential morphology are represented by a pacer located at the domain's boundary, while mechanical stimuli are distributed within the spatial domain and affect the action potential by altering intracellular calcium kinetics. Alternation of action potential is described by the small amplitude of alternans parabolic partial differential equation (PDE). Spatially uniform unstable steady-state of the alternans amplitude PDE is stabilized by optimal control methods through boundary and spatially distributed actuation. Mixed boundary and spatially distributed actuation is manipulated by a finite dimensional linear quadratic regulator (LQR) in the full-state feedback control structure and in a compensator design with a Luenberger-type observer, and it achieves exponential stabilization in a finite size tissue cable length. The proposed control problem formulation and the performance and robustness of the closed-loop system under the proposed linear controller are evaluated through simulations.**

Index Terms: **Cardiac mechano-electric feedback (MEF), Dissipative parabolic PDEs, LQR, State/output feedback control.**

I. INTRODUCTION

Sudden cardiac death and ventricular fibrillation are believed to be linked to the alternation of the electric activity of the myocardium. Electric activity in the heart is the consequence of propagation of electric waves caused by the exchange of ionic species between intracellular and extracellular spaces which is reflected in changes in the membrane potential of the myocardium cells. Electric wave propagation in myocardium belongs to the class of transport-reaction processes which are characterized by significant spatial variations due to the coupling of underlying diffusion and nonlinear dynamics phenomena. Hence, it has been shown that when cardiac tissue is stimulated at short pacing rates, the duration of electrical excitation varies from beat to beat, and it is manifested as a variation in the action potential duration (APD). These beat-to-beat oscillations are referred to as "alternans", see Fig.1.

Annihilation of detrimental alternans may represent an effective antiarrhythmic strategy and it has been addressed
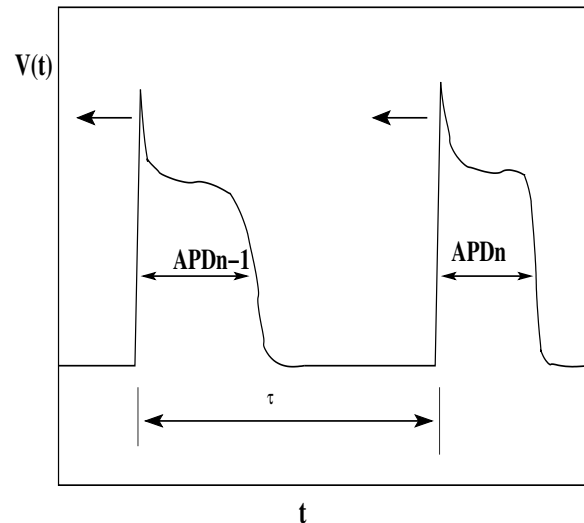

Fig. 1. Schematic time course of the transmembrane potential at a point along the cable with APD alternans, where the amplitude of alternans $a(\zeta, t)$ is defined as $a(\zeta, n) = (APD_{n,\zeta} - APD_{n-1,\zeta})(-1)^n$ with n being the beat number and $t = n\tau$ where τ is the basic beat length.

in the theoretical studies of Echebarria and Karma which demonstrated that alternans can be abolished only in a small portion of tissue by applying modulated feedback gain which perturbs the fixed pacing period and can be produced by consecutive APD measurements at the pacing site [18]. Control of this type belongs to the class of boundary control realizations since the pacing site is at the boundary of the domain which undergoes stabilization. Current assessment is that the applied pacing control stabilization of alternans is not successful due to limited ability of the applied pacing boundary input to alter the APD length away from the pacing site which has been demonstrated by theoretical and experimental works [18], [9], [25], [16].

An independent from pacing way to change the cell's electrical activity is to apply mechanical stimuli. In recent experimental and theoretical studies [23], [26], [24], [7], [3], it has been demonstrated that stretch-induced changes of myocardium cell length alter the electric activity through stretch-activated channels and by modulation of intercellular calcium kinetics. Namely, the kinetics of intercellular calcium is primarily responsible for the link among electrical and mechanical properties of the cell since binding

---

† Corresponding author. Email: `stevand@seas.ucla.edu`

of the intercellular calcium ions with contractile proteins provides a local mechanism of mechanic contractile act. Motivated by these findings, in this work stretch-based mechanical perturbation, which does not belong to the type of superthreshold stimuli, alters the intercellular calcium kinetics by which the cells electrical activity is modulated [7]. The stretch-based mechanical perturbation is spatially distributed within the myocardium tissue, and when paired with boundary applied pacing, it can provide a mixed boundary-spatially distributed mechano-electric perturbation that may, by mechanisms of mechano-electric feedback, lead to successful cardiac alternans annihilation. Boundary actuation is represented by the alternation of the pacing period at the boundary of the domain and it is realized by placing an electrode at the cardiac muscle. Spatially distributed actuation is associated with mechano-electric feedback (MEF), as a result of stretch-based mechanical perturbations on the tissue through stretch-activated and stretch-modulated ionic currents among which the calcium current is the most important one in the mechano-electric coupling mechanism. Spatially distributed mechanical stretch actuation can be easily realized by sewing the micro-electro-mechanical-based built patch to the epicardial myocardial tissue. Therefore, a mixed boundary and spatially distributed mechano-electric applied control is a new promising way to novel cardiac altenans annihilation therapy.

A small amplitude of alternans equation that was derived by Echebarria and Karma [18] obeys the form of parabolic partial differential equations (PDEs) that model diffusion-convection-reaction processes [29], [11]. Typically, systems described by parabolic PDEs admit an abstract evolutionary form on an appropriate functional space, and in the case of linear parabolic PDEs, the spatial differential operator is characterized by a spectrum that can be partitioned into a finite (possibly unstable) slow part and an infinite dimensional stable fast complement [21]. Hence, the traditional approach to control parabolic PDEs is to stabilize the unstable slow modal states via feedback, while the infinite dimensional stable modal complement remains stable under the applied feedback control structure.

Within the theory of control of parabolic PDEs, this work focuses on the subset of mixed boundary/distributed control problems for linear parabolic PDEs. In this area, significant research has been carried out in the works of Fattorini [20], Triggiani [28], Curtain [12], Christofides [10] and Emirsjlow and Townley [19], wherein necessary conditions for the stabilization under state and output feedback control have been defined. More recent results on the boundary control of distributed parameter systems include the use of singular functions for identification and control [8], boundary control of nonlinear distributed parameter systems by means of static and dynamic output feedback regulation [5], development of boundary feedback control laws based on the backstepping methodology [4] and model predictive methodology that includes input and state constraints in

the boundary/distributed control design [14], [15]. Building on these already developed control methods, the issue of stabilization of cardiac alternans by boundary and distributed applied actuation needs to be explored as a possible antiarrhythmic strategy.

In this paper, mixed boundary and distributed stabilization of small amplitude of the alternans equation described by a linear parabolic PDE by optimal control methods is demonstrated. Linear parabolic PDE of amplitude of alternans is defined as a mixed abstract boundary/distributed control problem in a well defined functional space. The analysis demonstrates that the spatial operator of the amplitude of alternans PDE is a Sturm-Liouville type operator, which possesses a few unstable modes that can be stabilized by means of boundary and distributed feedback control. Namely, only few unstable modes are exponentially stabilized by a full-state feedback linear quadratic regulator (LQR), while the remaining infinite-dimensional complement remains stable under the applied feedback controller. In the case of output feedback control, a Luenberger-type observer is integrated with the LQR control law to achieve exponential stabilization of the alternans amplitude PDE. In simulation studies, the relevant model of the Beeler Reuter cardiac cell is considered in order to obtain parameters of the amplitude of alternans equation. Successful stabilization by means of optimal boundary/distributed control of small amplitude of alternans is demonstrated and the effect of measurement noise and uncertainty/nonlinearities on the performance of the proposed controller is examined.

II. Preliminaries

The equation which describes small amplitude oscillations of the APD equation was developed by Echebarria and Karma [18], [17], and for one-dimensional $\zeta \in [0, l]$ case, the amplitude of alternans parabolic PDE takes the following form:

$$\tau_c \frac{\partial a(\zeta, t)}{\partial t} = D_a^2 \frac{\partial^2 a(\zeta, t)}{\partial \zeta^2} - w \frac{\partial a(\zeta, t)}{\partial \zeta} + \sigma a(\zeta, t) -$$

$$ga(\zeta, t)^3 - \frac{1}{\Lambda} \int_0^\zeta a(\bar{\zeta}, t) d\bar{\zeta} + h \sum_{i=1}^n b_{d_i}(\zeta) u_{d_i}(t) \quad (1)$$

$$\frac{\partial a(0, t)}{\partial \zeta} = a(0, t) + u(t)$$

$$\frac{\partial a(l, t)}{\partial \zeta} = 0 \quad (2)$$

$$y(t) = \int_0^l c(\zeta) a(\zeta, t) d\zeta \quad (3)$$

The parameters D_a and w are taken to be $D_a \approx \sqrt{D * APD_c}$ and $w \approx 2D/c_v^*$ where D is the voltage diffusion among the cells in the ionic model [2], APD_c is the APD evaluated at the bifurcation point, τ_c is the basic pacing cycle length at the bifurcation point, and c_v^* is the propagation speed of the wave front at the bifurcation point at which alternans start to emerge [18]. The parameter σ is the growth rate of alternans at the onset of period

doubling oscillations in the APD, while the parameter g is the nonlinear stabilizing contribution (see [17] for exact derivation of σ and g). The integral term in the Eq.1 reflects the contribution of the perturbation of the basic pacing cycle length on the amplitude of alternans. The parameter h represents the correlation that relates the changes in the intracellular calcium dynamics due to mechanical perturbations with respect to the alternans amplitude. In this analysis, the exact length and timing of the stretch activated excitation is not provided and the assumption is that stretch actuation is mainly manifested by the modulation of the intracellular calcium dynamics which is reflected in the changes in the APD morphology.

The amplitude of alternans PDE of Eqs.1-2 is linearized around the spatially-uniform unstable steady state ($a(\zeta, t) = 0$). We assume that alternans are slowly varying from the beat-to-beat in the proximity of the bifurcation point. We consider the case when alternans start to emerge and since alternans dynamics is described by a nonlinear bistable equation, a first approximation is given by the linearized amplitude of alternans equation. Further, the integral term in the Eq.1 that reflects the contribution of the perturbation of the basic pacing cycle length on the amplitude of alternans, in the context of control of relevant cardiac tissue size is negligible and can be neglected (the parameter $\Lambda \approx 45 - 50 cm$) [18]. See the simulation section for results, demonstrating that the use of the linearized model for controller design is adequate in the sense that a controller that is designed on the basis of the linearized PDE stabilizes the full model of Eqs.1-2.

In the ensuing text, the linearized amplitude of alternans PDE is considered and it can be formulated as a mixed abstract boundary/distributed control problem:

$$\dot{a}(t) = \mathcal{F}a(t) + \mathcal{B}_d u_d(t), \quad t \geq 0, \ a(0) = a_0, \quad (4)$$
$$\mathcal{B}a(t) = u(t)$$
$$y(t) = \mathcal{C}a(t)$$

where $\mathcal{F} : \mathcal{D}(\mathcal{F}) \subset \mathcal{W} \mapsto \mathcal{W}$, $\mathcal{B}_d \in \mathcal{L}(U_d, \mathcal{W})$, $\mathcal{B} : \mathcal{D}(\mathcal{B}) \subset \mathcal{W} \mapsto U$ satisfies $\mathcal{D}(\mathcal{F}) \subset \mathcal{D}(\mathcal{B})$, and U, U_d and $\mathcal{W}([0,l];t)$ are well-defined Sobolev spaces, with the state $a(\cdot, t) = \{a(\zeta, t), 0 \leq \zeta \leq l\} \in \mathcal{W}([0,l];t)$ [12], t is the time variable, $u(t) \in \mathbb{R}$ is the control input at the boundary, and $u_d(t)$ is the spatially distributed input. $L_2(0,l)$ denotes the Hilbert space of measurable square-integrable real-valued functions $f : [0,l] \to \mathbb{R}$, $\int_0^l |f(\zeta)|^2 d\zeta < \infty$, with weighted inner product and norm on $L_2(0,l)$, defined by $(f,g)_{\eta, L_2} = \int_0^l \eta f(\zeta) g(\zeta) d\zeta$ and $\|f\|_2 = \sqrt{(f,f)_{\eta, L_2}}$. Associated with Eq.4 is the operator $\mathcal{F}$ which is given by:

$$\mathcal{F}\phi(\zeta) = \left[D_a^2 \frac{d^2}{d\zeta^2} - w\frac{d}{d\zeta} + \sigma \right] \phi(\zeta) \quad (5)$$

with the domain defined by:

$$\mathcal{D}(\mathcal{F}) = \{\phi(\zeta) \in L_2(0,l) : \phi(\zeta), \phi(\zeta)', are \ abs. \ cont.,$$
$$\mathcal{F}\phi(\zeta) \in L_2(0,l), \ and \ \phi(l)' = 0\} \quad (6)$$

while the input operator of spatially-distributed control actuation is given by:

$$\mathcal{B}_d u_d(t) = h \sum_{i=1}^{n} b_{d_i}(\zeta) u_{d_i}(t) \quad (7)$$

where $b_{d_i}(\zeta) = \frac{1}{2\epsilon} 1_{[\zeta_{d_i} - \epsilon, \zeta_{d_i} + \epsilon]}(\zeta) \in L_2(0,l)$, (this notation means that $b_{d_i}(\zeta) = \frac{1}{2\epsilon}$ for $\zeta_{d_i} - \epsilon \leq \zeta \leq \zeta_{d_i} + \epsilon$ and $b_{d_i}(\zeta) = 0$ elsewhere). The output operator is defined by a sensor function as $c(\zeta) = \frac{1}{2\epsilon} 1_{[\zeta_c - \epsilon, \zeta_c + \epsilon]}(\zeta) \in L_2(0,l)$, and it is given by:

$$y(t) = (c(\zeta), a(\zeta, t)) = \mathcal{C}a(t) \quad (8)$$

The boundary operator $\mathcal{B} : L_2(0,l) \mapsto \mathbb{R}$ and its domain are given by:

$$\mathcal{B}\phi(\zeta) = \frac{d\phi(0)}{d\zeta} - \phi(0), \quad with \ \mathcal{D}(\mathcal{F}) \subset \mathcal{D}(\mathcal{B}) \quad (9)$$

In order to define a mixed abstract boundary/distributed control problem it is necessary to introduce a new operator $\mathcal{A}$ which is defined by:

$$\mathcal{A}\phi(\zeta) = \mathcal{F}\phi(\zeta) \quad and \quad \mathcal{D}(\mathcal{A}) = \mathcal{D}(\mathcal{F}) \cap ker(\mathcal{B}) =$$
$$\{\phi \in L_2(0,l) : \phi(\zeta), \phi(\zeta)' \ are \ abs. \ cont.,$$
$$\mathcal{A}\phi(\zeta) \in L_2(0,l), \ \phi'(0) = \phi(0) \ and \ \phi'(l) = 0\}$$
$$(10)$$

where $\mathcal{A}$ is the infinitesimal generator of a strongly continuous semigroup on $\mathcal{W}$. An assumption made here is that there exists a function $B(\zeta)$ so that for all $u(t)$, $Bu(t) \in \mathcal{D}(\mathcal{F})$ and the following holds:

$$\mathcal{B}Bu(t) = u(t), \quad u(t) \in U \quad (11)$$

The existence of B together with the assumption that the input $u(t) \in \mathbf{C}^2([0,t];U)$ and $u_d(t) \in \mathbf{C}^1([0,t];U_d)$ are sufficiently smooth, yield the following well-posed abstract differential equation:

$$\dot{p}(t) = \mathcal{A}p(t) + \mathcal{F}Bu(t) - B\dot{u}(t) + \mathcal{B}_d u_d(t),$$
$$p(0) = p_0 \in \mathcal{D}(\mathcal{A}) \quad (12)$$
$$y(t) = \mathcal{C}p(t) + \mathcal{C}Bu(t)$$

which has a well defined mild solution due to the boundedness of linear operators B and $\mathcal{F}B$, and due to the fact that $\mathcal{A}$ is the infinitesimal generator of a C_0-semigroup. Eq.12 and Eq.4 are related by the following transformation $p(t) = a(t) - Bu(t)$. As the abstract evolutionary equation of Eq.12 includes in its expression a derivative of the control term, it is reformulated on the extended state space $\mathcal{W}^e := \mathcal{W} \bigotimes U$, as $a^e(t) = [u(t) \ p(t)]'$ and together with $\tilde{u}(t) = \dot{u}(t)$ yields:

$$\dot{a}^e(t) = \begin{pmatrix} 0 & 0 \\ \mathcal{F}B & \mathcal{A} \end{pmatrix} a^e(t) +$$
$$\begin{pmatrix} I & 0 \\ -B & \mathcal{B}_d \end{pmatrix} \begin{pmatrix} \tilde{u}(t) \\ u_d(t) \end{pmatrix} \quad (13)$$
$$a^e(0) = [u(0) \ p(0)]' = a_0^e$$
$$y^e(t) = [\mathcal{C}B \ \mathcal{C}] a^e(t)$$

The operator $\mathcal{A}^e = (0\ 0; \mathcal{F}B\ \mathcal{A})$ with domain $\mathcal{D}(\mathcal{A}^e) = \mathcal{D}(\mathcal{A}) \bigotimes U$ is the infinitesimal generator of a C_0-semigroup on $\mathcal{W}^e$. The Riesz spectral operator $\mathcal{A}$ generates a C_0–strongly continuous semigroup $\mathcal{T}(t)$ given by:

$$\mathcal{T}(t) = \sum_{n=0}^{\infty} e^{\lambda_n t} \left(\cdot, \phi_n(\zeta) \right) \psi_n(\zeta) \tag{14}$$

so that $\sup\limits_{n \geq 1} Re(\lambda_n) \leq \infty$, where λ_n $\{n \geq 1\}$, are simple eigenvalues of $\mathcal{A}$, and $\phi_n(\zeta)$ and $\psi_n(\zeta)$ are the eigenfunctions of $\mathcal{A}$ and $\mathcal{A}^*$, respectively, so that the inner product $(\phi_n(\zeta), \psi_m(\zeta))_{L_2} = \delta_{nm}$ holds. The eigenvalue problem of the Sturm-Liouville operator given by Eq.5 and Eq.10 can be easily solved [12]. Namely, the operator $\mathcal{A}$ is given for any function in the domain $\mathcal{D}(\mathcal{A})$ by:

$$\mathcal{A}\phi(\cdot) = \frac{1}{\rho(\cdot)} \frac{d}{d\zeta} \left[p(\cdot) \frac{d\phi}{d\zeta}(\cdot) \right] + q(\cdot)\phi(\cdot) \tag{15}$$

where $\rho(\zeta) := e^{-\frac{w}{D_a^2}\zeta}$, $p(\zeta) := D_a^2\rho(\zeta)$, $q(\zeta) := \sigma$ which are continuously differentiable functions on $[0, l]$. The spectrum of eigenvalues of the operator $\mathcal{A}$ is $\Omega(\mathcal{A})$ and consists of isolated eigenvalues with finite multiplicity and it is given as:

$$\lambda_n = \sigma - D_a^2 \left[\alpha_n + \frac{w^2}{4D_a^4} \right], \ \ 0 < \alpha_n < \alpha_{n+1}, \ \ n \geq 1 \tag{16}$$

where α_n is the solution to the following transcendental equation:

$$tan(\sqrt{\alpha}L) = \frac{\sqrt{\alpha}}{\alpha - \frac{w}{2D_a^2}\left[1 - \frac{w}{2D_a^2}\right]} \tag{17}$$

while the eigenfunctions for all $n \geq 1$, are given by:

$$\phi_n(\zeta) = A_n e^{\frac{w}{2D_a^2}\zeta} \left[cos(\sqrt{\alpha_n}\zeta) + \right.$$
$$\left. (1 - \frac{w}{2D_a^2})\frac{1}{\sqrt{\alpha_n}} sin(\sqrt{\alpha_n}\zeta) \right] \tag{18}$$

and the adjoint eigenfunctions by $\psi_n(\zeta) = \phi_n^*(\zeta) = \phi_n(\zeta)e^{-\frac{w}{D_a^2}\zeta}$, where A_n are nonzero constants which are calculated by the orthogonality condition $(\phi_n(\zeta), \phi_m^*(\zeta))_{w/D_a^2, L_2} = \delta_{nm}$. The semigroup $\mathcal{T}(t)$ growth bound is given by $\omega_0 = \sup\limits_{n \geq 1} Re(\lambda_n) \leq \infty$ and the following characterization of the operator $\mathcal{A}$ that generates the operator $\mathcal{T}(t)$ is given by the Hille-Yoshida theorem [12], $\|\mathcal{T}(t)\| \leq Me^{\omega_0 t}$ for a $M > 0$.

Remark 1: The approximate controllability of mixed boundary/distributed controlled system of Eq.13 can be assured by checking that the following condition holds for all $n \geq 1$,

$$rank[(\mathcal{F}B(\zeta) - \lambda_n B(\zeta), \phi_n(\zeta))_{\frac{w}{D_a^2}, L_2} \ (\mathcal{B}_d, \phi_n(\zeta))_{\frac{w}{D_a^2}, L_2}] = 1 \tag{19}$$

where the first entry corresponds to the boundary actuation related condition of approximate controllability,

while the second entry refers to approximate controllability of spatially distributed actuation. In the same vein, the condition of approximate observability for the boundary/distributed controlled problem holds if the $rank[(\mathcal{C}(B(\zeta) + I), \phi_n(\zeta))] = 1$ holds for $n \geq 1$. The approximate controllability and observability conditions of boundary/distributed controlled system are transformed from their standard forms due to the boundary transformation [12].

III. OPTIMAL CONTROLLER DESIGN

The operator $\mathcal{A}^e$ spectrum is partitioned into a finite dimensional unstable part $\Omega^+(\mathcal{A}^e)$ and an infinite dimensional stable complement $\Omega^-(\mathcal{A}^e)$, $\Omega(\mathcal{A}^e) = \Omega^+(\mathcal{A}^e) \cup \Omega^-(\mathcal{A}^e)$. The finite dimensional LQR problem for the finite dimensional state given by $a_u^e(t) = [u(t)\ p_u(t)]'$ and boundary/distributed actuation $\bar{u}(t) = [\tilde{u}(t)\ u_d(t)]'$ is formulated in the following form:

$$\min_{\bar{u}} J(a_u^e(0); \bar{u}) = \int_0^{\infty} \left(a_u^e(t)'Q a_u^e(t) + \bar{u}(t)'R\bar{u}(t) \right) dt \tag{20}$$
$$s.t. \ \dot{a}_u^e(t) = \mathcal{A}_u a_u^e(t) + \mathcal{B}_u \bar{u}(t) \tag{21}$$

where $\mathcal{A}_u$ and $\mathcal{B}_u$ are matrices that correspond by their dimensions to the dimensions of an unstable eigenspace $\Omega^+(\mathcal{A}^e)$, and Q and R are positive semidefinite and definite matrices, respectively. The resulting linear optimal controller is $\bar{u}(t) = -\frac{1}{2}R^{-1}\mathcal{B}_u'P a_u^e(t) = -\mathcal{K}a_u^e(t)$, where P is a positive definite solution to the LQR-ARE [6]:

$$0 = \mathcal{A}_u'P + P\mathcal{A}_u + Q - P\mathcal{B}_u R^{-1}\mathcal{B}_u'P \tag{22}$$

Standard Lyapunov based analysis of stabilization of unstable modes $a_u^e(t)$ by LQR state feedback can be demonstrated by considering the following standard control Lyapunov function (CLF), $V(t) = a_u^e(t)'P a_u^e(t)$, so that:

$$\begin{aligned} \dot{V}(t) &= \frac{d}{dt}[a_u^e(t)'P a_u^e(t)] \\ &= a_u^e(t)' \left(\mathcal{A}_u'P + P\mathcal{A}_u - P\mathcal{B}_u R^{-1}\mathcal{B}_u'P \right) a_u^e(t) \\ &= -a_u^e(t)'Q a_u^e(t) < 0 \end{aligned} \tag{23}$$

From Eq.23, it can be concluded that the unstable modes are optimally stabilized and due to the cascaded interconnection between unstable and stable modal states, once the unstable states are stabilized under the stabilizing feedback law, $a_u^e(t) \rightarrow 0$ and $\bar{u}(t) \rightarrow 0$, the stable infinite modal states evolution is only driven by the zero-input dynamics which renders exponential stability of the infinite dimensional closed-loop system. The approximate controllability of the mixed boundary/distributed control system can be assured by checking that the condition given by Eq.19 holds. In the formulation of the LQR control law given by Eqs.20-21 the associated weights given by Q and R matrices represent weights on the state evolution $p(t)$, control input evolution $u(t)$ and $u_d(t)$, and derivative of boundary control input $\tilde{u}(t)$. The first diagonal term in the matrix Q represents the weight that is associated with $u(t)$, while the remaining nonzero terms are weights on

modal states $p(t)$. The term R consists of the weight on the derivative of the input and weights on the distributed control input.
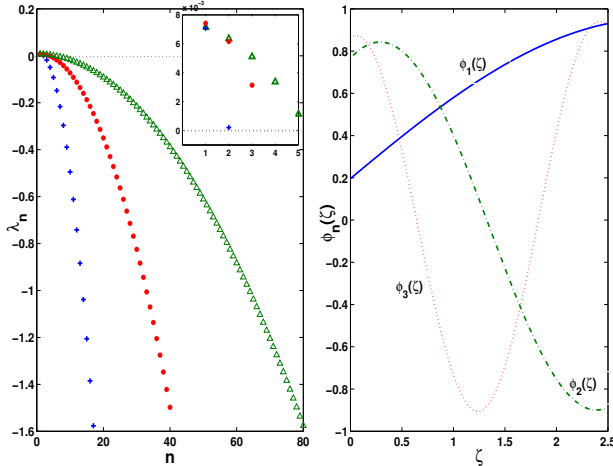

Fig. 2. Left plot: Distribution of eigenvalues on the basis of Eq.16 for different lengths of the cable (1 cm ($*$), 2.5 cm ($\cdot$), 5 cm ($\triangle$)). Right plot: First three eigenfunctions of unstable eigenmodes of the operator $\mathcal{A}$ given by Eq.18 for the cable length equal to 2.5 cm.

In the case where state feedback control can not be realized, it is natural to extend the controller synthesis by incorporating an observer in the feedback structure. A state observer of the Luenberger type is considered [13]. The assumption of approximate observability is made [12], and the Luenberger observer is constructed as,

$$\dot{\hat{a}}_u^e = \mathcal{A}_u \hat{a}_u^e(t) + \mathcal{B}_u \tilde{u}(t) - \mathcal{L}(y(t) - \mathcal{C}_u \hat{a}^e(t)) \qquad (24)$$

where $\mathcal{C}_u$ is the matrix of appropriate dimensions corresponding to the dimensions of the unstable eigenspace $\Omega^+(\mathcal{A})$ and the number of measurement sensors. Finally, under the assumption of exponential stabilizability and detectability of $(\mathcal{A}_u, \mathcal{B}_u)$ and $(\mathcal{A}_u, \mathcal{C}_u)$, respectively, there exist $\mathcal{K}$ and $\mathcal{L}$ so that $\mathcal{A}_u + \mathcal{B}_u\mathcal{K}$ and $\mathcal{A}_u + \mathcal{C}_u\mathcal{L}$ are exponentially stable. The resulting output feedback controller enforces exponential stability in the linearized finite-dimensional closed-loop system.

Remark 2: It is of importance to address the issue of noise in the framework of the compensator design. Propagation of the electric wave front in the myocardium is approximately around 65 cm/sec which implies that a small noise introduced at the boundary where the control is applied may generate perturbations that will propagate and form a standing wave solution, which is usually, in a crude approximation, a linear combination of the unstable eigenspace modes' eigenfunctions. This effect is indeed observed in the experimental realization of pacing protocols that measure the amplitude of alternans at the pacing site and apply a self-referencing gain feedback modulation of the basic pacing period at the pacing site [9]. In simulation studies in the following section, it is demonstrated that the noise level that will produce a substantial deviation of the state $a(n, \zeta)$ from zero under a compensator in use in the

closed loop is very low.

Remark 3: Although the optimal stabilization of unstable modes of the finite dimensional subsystem via state feedback control achieves the exponential stabilization of infinite dimensional state, it neglects the influence of a feedback gain on the remaining set of eigenmodes in a sense that the feedback gain may excite higher modes of the operator $\mathcal{A}$ and produce high gain that amplifies the higher modes evolution. This phenomenon is referred to as spillover effect and it is analyzed in [1], [22]. This phenomenon is reflected in a possible high excursion of the state from the spatially uniform equilibrium state $a(\zeta, t) = 0$ far from the boundary where the control is applied before the state $a(\zeta, t)$ eventually settles to zero.
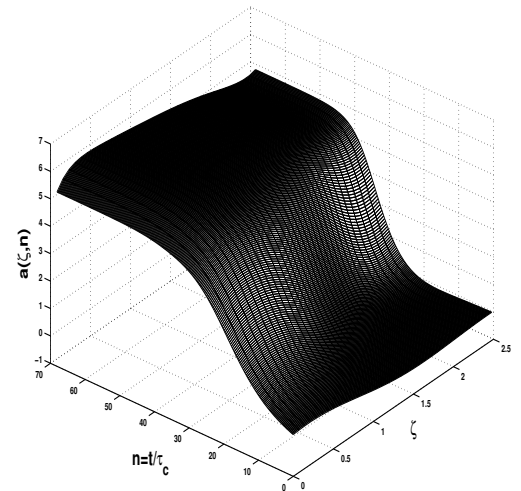

Fig. 3. Open-loop evolution of amplitude of alternans Eqs.1-2.

IV. SIMULATION STUDY

The parabolic PDE of Eqs.1-2 is considered. The parameters D_a, w, σ, h, g and Λ are obtained from the Beeler Reuter model of a cardiac cell [2]. The critical basic pacing cycle at the bifurcation point where the onset of alternans emerges is at $\tau_c = 275$ $msec$. The following values of $D_a^2 = 0.1732$ cm^2 with voltage diffusion being $D = 10^{-3} cm^2/msec$, $w = 0.0107$ cm and $\sigma = log(8)$, and $h = -0.0201$ $msec$ are calculated. The parameters associated with the nonlinear and integral term are $\Lambda = 49$ and $g = 0.0739$. The spectrum of the operator $\Omega(\mathcal{A})$ is calculated using Eqs.16-17 and it reveals different distributions of eigenvalues for different cable lengths. Namely, for $l = 2.5$ that is considered as a study case length of the cable under the optimal control law of Eqs.20-21, the first three eigenvalues of the operator $\mathcal{A}$ are unstable ($\lambda_1 = 0.007429, \lambda_2 = 0.0061607, \lambda_3 = 0.0031352$), while the remaining infinite eigenvalues are stable, see Fig.2. The eigenfunctions corresponding to the first three

eigenvalues are given in Fig.3. It can been seen from Fig.2 that an increase in the cable length increases the number of unstable modes of the operator $\mathcal{A}$ which need to be stabilized in order to achieve stabilization along the entire cable length. Moreover, Fig.2 demonstrates that increase in the cable length promotes more convective nature of the underlying PDE, since the necessary "gap" condition that provides that consecutive stable eigenvalues have a sufficiently large difference among themselves (see the appendix of [10], and [27]), fails to hold. This condition is difficult to satisfy in systems with strong convective terms and/or a small diffusion parameter. The parabolic
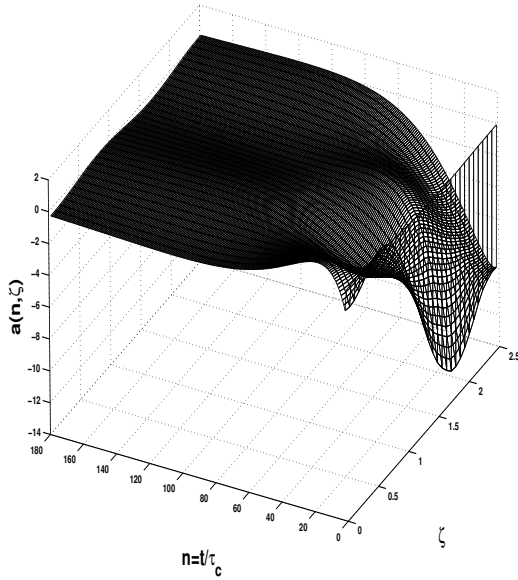

Fig. 4. Boundary/distributed stabilization of the linearized alternans amplitude PDE under the state-feedback control law $\bar{u}(t) = -Ka_u^e(t)$, where $a(\zeta,t) = \sum_{i}^{39} a_i(t)\phi_i(\zeta)$ and with initial condition $a_{u2}^e(0) = 0.4$, $a_{u3}^e(0) = 0.15$ and $a_{u4}^e(0) = 0.35$.

PDE of Eqs.1-2 is linearized around the spatially-uniform unstable steady state $a(\zeta,0) = 0$ and the integral term is neglected in order to allow for LQR controller synthesis. A high-order finite-dimensional approximation of the infinite dimensional abstract boundary/distributed control problem given by Eq.13 is first obtained by considering 39 eigen-functions $a(\zeta,t) = \sum_{i}^{39} a_i(t)\phi_i(\zeta)$, and it is given by:

$$\dot{a}^e(t) = \bar{\mathcal{A}}^e a^e(t) + \bar{\mathcal{B}}^e \tilde{u}(t) \qquad (25)$$
$$y_i(t) = \bar{\mathcal{C}}^e a^e(t) \qquad (26)$$

where $\bar{\mathcal{A}}^e$, $\bar{\mathcal{B}}^e$ and $\bar{\mathcal{C}}^e$ are matrices of the following dimensions (40×40), $(40 \times (\#$ of spatially distributed actuators$))$, $((\#$ of spatially distributed sensors$) \times 40)$, respectively, with 4 sensors used at $c(\zeta,\zeta_{ci}) = \frac{1}{2\epsilon}1_{[\zeta_{ci}-\epsilon,\zeta_{ci}+\epsilon]}(\zeta)$, where $\zeta_{ci} =$

[0.0501 1.0772 1.6533 2.3046], while spatially distributed mechanical actuation $b_d(\zeta,\zeta_{d_i}) = \frac{1}{2\epsilon}1_{[\zeta_{d_i}-\epsilon,\zeta_{c_i}+\epsilon]}(\zeta)$, is placed at $\zeta_{d_i} = $ [1.6250 2.2250]. Standard Galerkin

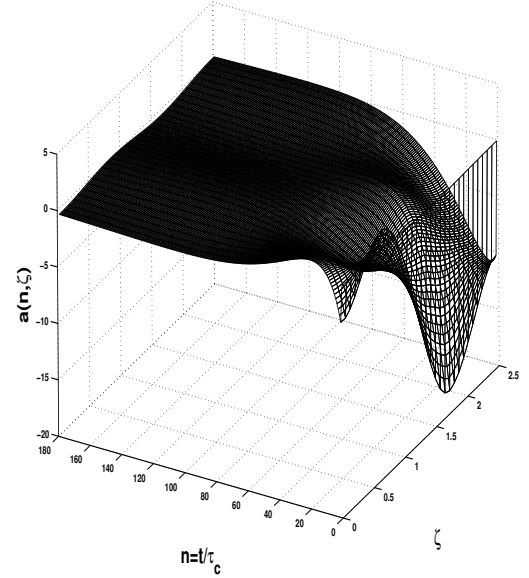Fig. 5. Boundary/distributed stabilization of the linearized alternans amplitude PDE under linear output feedback control, where $a(\zeta,t) = \sum_{i}^{39} a_i(t)\phi_i(\zeta)$ and with initial condition $a_{u2}^e(0) = 0.21$, $a_{u3}^e(0) = 0.4$ and $a_{u4}^e(0) = 0.2$.

method is performed (see for details [10]), where modal finite dimensional approximation of Eqs.1-2 is obtained by taking weighted inner product on $L_2(0,l)$ with adjoint eigenfunctions $(a(\zeta,t),\phi_j^*(\zeta))_{w/D_a^2,L_2}$. Function $B(\zeta) \in \mathcal{D}(\mathcal{F})$ is selected to satisfy the following condition $\mathcal{B}Bu(t) = u(t)$ and it is chosen to be $B(\zeta) = \zeta - \frac{1}{2l}\zeta^2$. In the extended space $\mathcal{D}(\mathcal{A}^e) = \mathcal{D}(\mathcal{A}) \bigoplus U$, the entries of finite dimensional matrices $\bar{\mathcal{A}}^e$, $\bar{\mathcal{B}}^e$ and $\bar{\mathcal{C}}^e$ are calculated as follows:

$$(\mathcal{F}B)_n = (-\frac{D_a^2}{l} - w(1-\frac{1}{l}\zeta) + \sigma(\zeta - \frac{1}{2l}\zeta^2), \phi_n^*(\zeta))_{w/D_a^2,L_2}$$
$$B_n = \left(\zeta - \frac{1}{2l}\zeta^2, \phi_n^*(\zeta)\right)_{w/D_a^2,L_2}$$
$$B_{dn} = (b_d(\zeta,\zeta_{ci}), \phi_n^*(\zeta))_{w/D_a^2,L_2}$$
$$C_{in} = \left((c(\zeta,\zeta_{ci}), \zeta - \frac{1}{2l}\zeta^2);\ (c(\zeta,\zeta_{ci}), \phi_n(\zeta))\right)_{w/D_a^2,L_2}$$

for $n \geq 1$ and $i = 1,\cdots,4$. Note that when the nonlinear and integral terms are considered, they can be computed within the Galerkin-discretization scheme as follows:

$$\mathcal{G}_n(t) = (ga(\zeta,t)^3, \phi_n^*(\zeta))_{w/D_a^2,L_2}$$
$$\mathcal{L}_n(t) = (\frac{1}{\Lambda}\int_0^l a(\bar{\zeta},t)d\bar{\zeta}, \phi_n^*(\zeta))_{w/D_a^2,L_2} \qquad .$$

To construct the linear model used for controller design, the first four unstable modal states of the model of Eq.25 are considered as follows:

$$a_u^e(t) = [u(t); p_1(t); p_2(t); p_3(t)]$$

with associated matrices which are of appropriate dimensions (4×4) in the case of $\bar{\mathcal{A}}_u = [0\ 0\ 0\ 0; (\mathcal{F}B)_1\ \lambda_1\ 0\ 0; (\mathcal{F}B)_2\ 0\ \lambda_2\ 0; (\mathcal{F}B)_3\ 0\ 0\ \lambda_3]$ (4×2) in the case of $\bar{\mathcal{B}}_u = [I\ 0; -B_1\ B_{d1}; -B_2\ B_{d2}; -B_3\ B_{d3}]$, with B_{d1}, B_{d2}, B_{d3} being (2×1) matrices, and (4×4) in the case of $\bar{\mathcal{C}}_u = [B(\zeta_{ci}); \phi_1(\zeta_{ci}); \phi_2(\zeta_{ci}); \phi_3(\zeta_{ci})]$, with $\bar{u}(t) = [\tilde{u}(t)\ u_d(t)]'$ and $\tilde{u}(t)$ being derivative of $u(t)$. The LQR regulator control law $\bar{u}(t) = -K a_u^e(t)$ is the solution of the following optimization problem:

$$\min_{\bar{u}} J(a_u^e(0); \bar{u}) = \int_0^{\infty} (a_u^e(t)'Q a_u^e(t) + \bar{u}(t)'R\bar{u}(t))\, dt \quad (27)$$

$$s.t.\ \dot{a}_u^e(t) = \bar{\mathcal{A}}_u a_u^e(t) + \bar{\mathcal{B}}_u \bar{u}(t) \quad (28)$$

which yields the following stabilizing gain

$$K = \begin{pmatrix} 3.136 & 0.7755 & 0.1967 & 0.06276 \\ 1403.5 & 24.1305 & 66.790 & 59.2839 \\ 995.30 & 38.431 & 123.71 & -61.4311 \end{pmatrix}$$

that places the unstable eigenmodes of the four-dimensional closed-loop system at the following locations $\lambda_{cl} = [-4.0508\ -0.0074\ -0.0062\ -0.0032]$ for the following values of matrices $Q^e = [q_u\ 0;\ 0\ q_a I]$ where $q_a = 0.01$ and I is the unitary matrix and $q_u = 0.0001$, where $R = diag\{R_u, R_{ud}\}$ with $R_u = 100$ and $R_{ud} = 0.0001$. Furthermore, the gain of the Luenberger observer of Eq.24 is calculated as the gain that places the observer eigenvalues at $\lambda_{\mathcal{LC}} = \lambda_{cl} - 2.5$ in order to ensure faster convergence of the observer dynamics compared to the systems dynamics. The control law $\tilde{u}(t) = -K a_u^e(t)$ is first applied to the linear finite dimensional approximation of Eqs.25-26 with 39 eigenfunctions and the solution is obtained by integrating the closed-loop system by an explicit Euler integration scheme where the time step is taken as $\triangle t = \frac{1}{4max|eig\{\Omega(\mathcal{A})^e\}|}$ so that numerical stability is ensured.

Complementary with Fig.4 is Fig.8 that shows the evolution of the control $u(t)$ applied at the boundary $\zeta = 0$ and spatially distributed $u_d(t)$ at $\zeta_{d_i} = [1.6250\ 2.2250]$. In the simulation study, it is demonstrated that the PDE state close to the boundary where control is applied undergoes large variations in the magnitude even for a relatively small excursion of initial conditions, which is due to the necessity to have the three unstable modes stabilized, see Fig.4-8. In the case of linear output feedback control with four point measurements, the successful stabilization of alternans is achieved in a similar manner as in the case of state-feedback stabilization, see Fig.5. As expected, it is observed that the state-feedback controller slightly outperforms the output-feedback controller, see Figs.5-8. In Fig.8 both dashed and solid lines converge to the same trajectory, as it takes initially some time for the state estimate to converge to the actual state. In addition, when the impact of noisy measurements is included in the output feedback controller implementation, our simulation studies, using the linearized PDE model, demonstrate that even a very small noise level results in substantial deviation of the state $a(n, \zeta)$
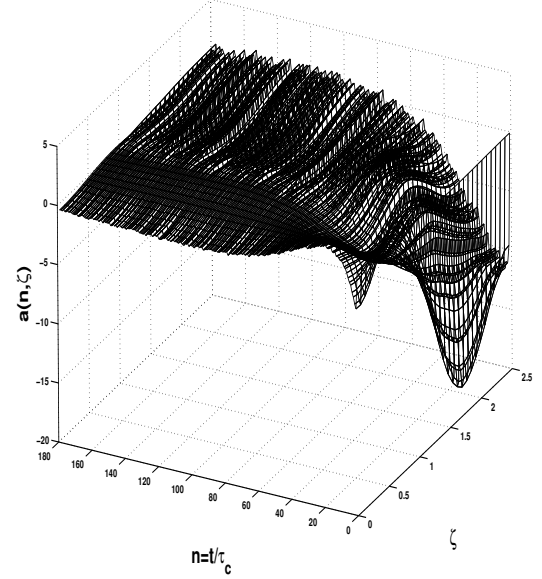

Fig. 6. Boundary/distributed stabilization of the linearized alternans amplitude PDE under linear output feedback control, with measurement noise $\varrho(t) \leq 0.001$ and with initial condition $a_{u2}^e(0) = 0.21$, $a_{u3}^e(0) = 0.4$ and $a_{u4}^e(0) = 0.2$.

from the zero solution. Namely, for noise of magnitude $\varrho(t) \leq 0.001$ that is directly added to $y(t)$ in Eq.24, we observe, see Fig.6 and Fig.8 (dotted and dashed lines of the input profiles almost coincide as the difference is only due to the additive measurement noise), that $a(n, \zeta)$ behaves like a near standing wave in space which oscillates around $a(n, \zeta) = 0$ with respect to time. This strongly advocates and confirms that the current realization of noisy stabilizing protocols can not inherently stabilize (i.e., set $a(n, \zeta) = 0$) alternans due to high sensitivity to noisy measurements used in the feedback controller.

Finally, in Figure 7, it can be seen that the stabilization of the spatially-uniform unstable steady state of the full non-linear model of Eqs.1-2 under the linear LQR control law is achieved. This result makes sense since essentially both the nonlinear and integral terms provide a stabilizing effect on the amplitude of alternans, which is also manifested in the faster convergence of the applied boundary and spatially distributed inputs to zero, see Fig.8.

V. Summary

The work focused on mixed boundary/spatially distributed control of the amplitude of alternans parabolic PDE using optimal control methods. This problem arises in the context of stabilization of cardiac alternans using mechano-electric feedback. The proposed control problem formulation and the performance and robustness of the closed-loop system were studied through simulations.
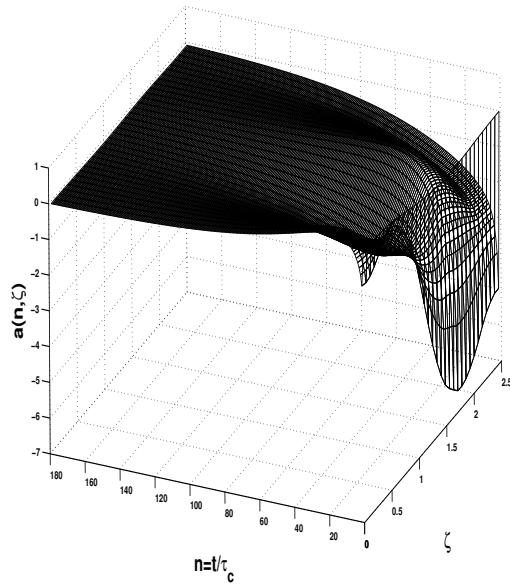
Fig. 7. Boundary/distributed stabilization of the nonlinear alternans amplitude PDE given by Eqs.1-2 under the linear LQR state-feedback control law $\bar{u}(t) = -Ka(t)$, and with initial condition $a_{u2}^e(0) = 0.21$, $a_{u3}^e(0) = 0.4$ and $a_{u4}^e(0) = 0.2$.
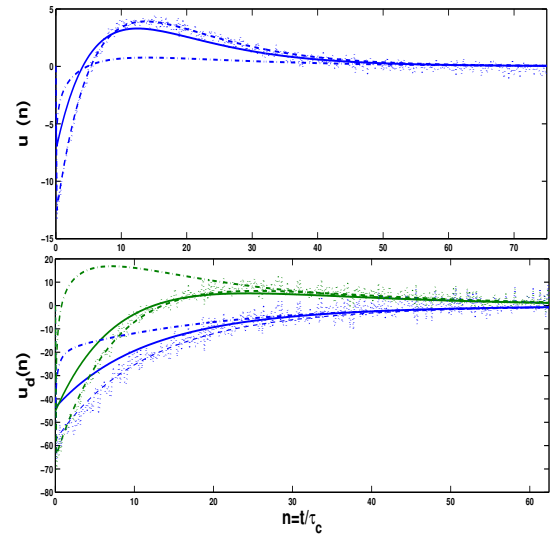

Fig. 8. Optimal control input computed by the state-feedback control law (solid-line– boundary input $u(n)$ and distributed input $u_d(n)$), by the output feedback control law (dashed-line– boundary input $u(n)$ and distributed input $u_d(n)$), by the output feedback control law with the additive noise (dotted-line– boundary input $u(n)$ and distributed input $u_d(n)$), applied to the linearized alternans amplitude PDE, and optimal control input under the LQR state-feedback control law applied to Eqs.1-2 (dashed-dotted-line– boundary input $u(n)$ and distributed input $u_d(n)$).

REFERENCES

[1] M. J. Balas. Active control of flexible systems. *J. Optim. Theory. Appl.*, 25:415–436, 1978.

[2] G. W. Beeler and H. Reuter. Reconstruction of the action potential of ventricular myocardial fibers. *Journal of Physiology*, 45:11911202, 1977.

[3] D. M. Bers. *Excitation-Contraction Coupling and Cardiac Contractile Force*. Kluwer Academic, 2001.

[4] D. M. Boskovic, M. Kristc, and W. Liu. Boundary control of an unstable heat equation via measurement of domain-averaged temperature. *IEEE Trans. Autom. Contr.*, 46:2022–2028, 2001.

[5] C. I. Byrnes, D. S. Gilliam, A. Isidori, and V. I. Shubov. Static and dynamic controllers for boundary controlled distributed parameter systems. *Proceedings of the 43rd IEEE Conference on Decision and Control*, pages 3324–3325, 2004.

[6] Willems J. C. Least squares stationary optimal control and the algebraic riccati equation. *IEEE Trans. Automat. Contr.*, 6:621–634, 1971.

[7] S. C. Calaghan, A. Belus, and E. White. Do stretch-induced changes in intracellular calcium modify the electrical activity of cardiac muscle? *Prog. Biophys. Mol. Biol.*, 82:81–95, 2003.

[8] S. Chakravarti and W. H. Ray. Boundary indentification and control of distributed parameter systems using singular functions. *Chem. Eng. Sci.*, 54:1189–1204, 1999.

[9] D. J. Christini, M. L. Riccio, C. A. Culianu, J. J. Fox, A. Karma, and R. F. Gilmour. Control of electric alternans in canine cardiac purkinje fibers. *Phys. Rev. Lett.*, 96:104101, 2006.

[10] P. D. Christofides. *Nonlinear and Robust Control of PDE Systems: Methods and Applications to Transport-Reaction Processes*. Birkhäuser, Boston, 2001.

[11] M. C. Cross and P. C. Hohenberg. Pattern formation outside of equilibrium. *Rev. Mod. Phys.*, 65:851, 1993.

[12] R. F. Curtain and H. Zwart. *An introduction to Infinite-Dimensional Linear Systems Theory*. Springer-Verlag, New York, 1995.

[13] D. Dochain. State observation and adaptive linearizing control for distributed parameter (bio)chemical reactors. *Int. J. Adapt. Control Signal Process.*, 15:633–653, 2001.

[14] S. Dubljevic and P. D. Christofides. Predictive control of parabolic PDEs with boundary control actuation. *Chem. Eng. Sci.*, 61:6239–6248, 2006.

[15] S. Dubljevic, N. H. El-Farra, P. Mhaskar, and P. D. Christofides. Predictive control of parabolic pdes with state and control constraints. *Inter. J. Rob. & Non. Contr*, 16:749–772, 2006.

[16] S. Dubljevic, S.-F. Lin, and P. D. Christofides. Studies on feedback control of cardiac alternans. *Comp. & Chem. Eng., in press*.

[17] B. Echebarria and A. Karma. Instability and spatiotemporal dynamics of alternans in paced cardiac tissue. *Phys. Rev. Lett.*, 88:208101, 2002.

[18] B. Echebarria and A. Karma. Spatiotemporal control of cardiac alternans. *Chaos*, 12:923–930, 2002.

[19] Z. Emirsjlow and S. Townley. From PDEs with boundary control to the abstract state equation with an unbounded input operator: A tutorial. *European Journal of Control*, 6:27–49, 2000.

[20] H. O. Fattorini. Boundary control systems. *SIAM Journal on Control*, 6:349–385, 1968.

[21] A. Friedman. *Partial Differential Equations*. Holt, Rinehart & Winston, New York, 1976.

[22] G. Hagen and I. Mezic. Spillover stabilization in finite-dimensional control and observer design for dissipative evolution equation. *SIAM J. Control Optim.*, 42:746–768, 2003.

[23] P. Kohl, P. Hunter, and D. Noble. Stretch-induced changes in heart rate and rhythm: clinical observations, experiments and mathematical models. *Prog. Biophys. Mol. Biol.*, 82:91–138, 1999.

[24] P. Kohl and U. Ravens. Cardiac mechano-electric feedback: past, present, and prospect. *Prog. Biophys. Mol. Biol.*, 82:3–9, 2003.

[25] S.-F. Lin and S. Dubljevic. Pacing real-time spatiotemporal control of cardiac alternans. *Proc. of the Amer. Cont. Conf., New York City, NY*, 600–606, 2007.

[26] O. E. Solovyova, N. A. Vikulova, P. V. Konovalov, P. Kohl, and V. S. Markhasin. Mathematical modeling of mechano-electric feedback in cardiomyocytes. *Russ. J. Numer. Anal. Math. Modelling*, 4:331–351, 2004.

[27] R. Temam. *Infinite-Dimensional Dynamical Systems in Mechanics and Physics*. Springer-Verlag, New York, 1988.

[28] R. Triggiani. Boundary feedback stabilization of parabolic equations. *Applied Mathematics and Optimization*, 6:201–220, 1980.

[29] Ray W.H. *Advanced Process Control*. McGraw-Hill, New York, New York, 1981.